Entanglement dynamics in a two-mode nonlinear bosonic Hamiltonian

2003 J. Phys. A: Math. Gen. 36 9737

(http://iopscience.iop.org/0305-4470/36/37/311)

INSTITUTE OF PHYSICS PUBLISHING JOURNAL OF PHYSICS A: MATHEMATICAL AND GENERAL

J. Phys. A: Math. Gen. **36** (2003) 9737–9754 PII: S0305-4470(03)57491-1

Entanglement dynamics in a two-mode nonlinear bosonic Hamiltonian

L Sanz, R M Angelo[1] and K Furuya

Instituto de Física 'Gleb Wataghin', Universidade Estadual de Campinas UNICAMP, Caixa Postal 6165, 13083-970, Campinas, SP, Brazil

E-mail: lilisanz@ifi.unicamp.br, renato@ifi.unicamp.br and furuya@ifi.unicamp.br

Received 16 December 2002, in final form 14 July 2003
Published 2 September 2003
Online at stacks.iop.org/JPhysA/36/9737

Abstract

An exactly solvable case of an interacting Hamiltonian of two bosonic modes is considered to study fundamental properties of the entanglement dynamics for coupled nonlinear oscillators. Such an interaction is of physical importance, either in a two-species Bose–Einstein condensate or in the case of two modes of electromagnetic fields interacting in Kerr media. The time-evolved state is obtained analytically for initial products of two Fock and two coherent states, and the purification times of the subsystems are determined. The possibility of dynamical generation of a quantum superposition state is discussed at such purification times. We also identify the existence of two regimes: the short time, *phase spread* regime where subsystem entropy rises monotonically and the *self-interference* regime where it oscillates and a purification phenomenon can be observed. Our results also show that the *break time* from the first regime to the second one becomes longer, as well as the purification and reversibility times, as the Planck constant becomes much smaller than a typical action in phase space.

PACS numbers: 42.50.Ct, 03.65.Ud, 42.50.Dv, 05.30.Jp

1. Introduction

Nowadays, it is widely accepted that quantum entanglement is an essential ingredient for the implementation of quantum information processing devices [1]. It is notable that until recently quantum information science was restricted to discrete, finite-dimensional Hilbert space elements, however, interest in continuous variables has been developing in various contexts:

[1] Present address: Universidade de São Paulo, Instituto de Física, Caixa Postal 66318, 05315-970, São Paulo, SP, Brazil.

from teleportation [2], cryptography [3] to cloning [4]. This is closely connected to the recent advances of enhancing nonlinear coupling via an electromagnetically induced transparency (EIT) mechanism [5] using a Bose–Einstein condensate, which has opened up possibilities of strong nonlinear interaction of ultra slow light pulses [6] of tiny energies belonging to different modes of electromagnetic fields [7, 8]. Considering these developments, it is important to understand the entanglement properties of the Kerr-type interaction particularly for Gaussian states, which are one of the kinds of states that can be generated by simple experimental devices such as beam splitters and phase shifters. Several optical schemes where two modes of electromagnetic field interact inside nonlinear Kerr media have been discussed in the literature [9, 10].

Another experimental achievement that has opened up possibilities of studying quantum coherence properties in a condensed matter system is the Bose–Einstein condensation (BEC) [11]. An extensive theoretical study has been done on a system of bimodal Josephson coupled BECs, allowing both interspecies and intra-species two-body collisions between atoms [12, 13]. Dynamical generation of entangled states has been discussed in a simple two-mode model system where bosons are restricted to occupy one of the two modes, each of which is a BEC with a different internal degree of freedom [14, 15]. Also, proposals to produce macroscopic superposition states based on the two-mode model where the two species are coupled via Josephson-type coupling has been discussed [16–18]. In these works, a certain parameter regime of the adjustable Josephson coupling of the two species (realized experimentally by a Raman transition) has been established for the formation of such states.

In the present work, we have studied the entanglement properties of a model describing a bipartite system of two bosonic degrees of freedom, an integrable version of two quartic oscillators [19, 20], coupled via a biquadratic interaction. Some possible realizations of these type of interactions are present in: a coupled cavity scheme with a Kerr medium [21, 22]; propagation of two electromagnetic field modes in a Mach–Zehnder interferometer [10]; or, more interestingly, an interacting two-mode BEC [23–25]. In the last case, under certain restricted conditions [11], an integrable version of the two-mode model system can show some complementary aspects of the dynamics of mode-entanglement discussed in [15].

The role of the nonlinearity of each of the subsystem oscillators is discussed, and shown to have some of the properties present in one degree of freedom such as collapses and revivals of the quadrature mean values of each bosonic mode. Also, this solvable model in which the nonlinearity is present can be used to understand the role of biquadratic interaction on the entanglement dynamics of initially coherent Gaussian states. Another case we have considered is Fock states for the initial disentangled state, showing several differences in the entanglement dynamics compared with the previous case.

The paper is organized as follows: In section 2, the model is introduced and the exact solutions for initially disentangled states, in the cases of Fock states and coherent states, are presented. Analytical expressions for the subsystem density operators and some mean values are calculated. Section 3 is reserved to present the exact subsystem entropies for both initial states, analysis of the conditions for purification, times of maximal entanglements. At the purification times, we also discuss the possibility of formation of superpositions of coherent states, or Schrödinger cat states. The semiclassical limit of the subsystem entropy is also discussed, examining its behaviour as the Planck constant is allowed to become much smaller than the typical action in phase space. A short comment based on numerical results is given in section 4 about a more realistic case where the nonlinear couplings are slightly different. Finally, in section 5 we present our conclusions, and in the appendix we present the details of the calculations of a mixture of Schrödinger cat states.

2. The model

The theoretical model consists of two bosonic lossless modes, described by the creation and annihilation operators $\hat{a}_k$ and $\hat{a}_k^\dagger$ ($k = 1, 2$). Each mode has a nonlinear interaction term of the form $\hat{a}_k^{\dagger 2}\hat{a}_k^2$ (Kerr interaction [20], intra-species collision) and the biquadratic interaction term (cross-Kerr interaction [22], interspecies collision term). Besides these nonlinear terms, a linear coupling interaction between the bosonic modes has been considered, which is the usual RWA coupling in optics [26] or internal Josephson coupling in BECs, leading to the following Hamiltonian:

$$\hat{H} = \sum_{k=1}^{2}\left[\hbar\omega_k\left(\hat{a}_k^\dagger\hat{a}_k + \frac{1}{2}\right)\right] + \hbar\lambda\left(\hat{a}_1^\dagger\hat{a}_2 + \hat{a}_1\hat{a}_2^\dagger\right) + \hbar^2 g_1\left(\hat{a}_1^\dagger\hat{a}_1\right)^2 + \hbar^2 g_2\left(\hat{a}_2^\dagger\hat{a}_2\right)^2 + 2\hbar^2 g_{12}\hat{a}_1^\dagger\hat{a}_1\hat{a}_2^\dagger\hat{a}_2. \tag{1}$$

Here, ω_k is the frequency of the kth mode, λ is the coupling associated with the bilinear interaction term, g_1, g_2 and g_{12} are the nonlinear coupling parameters. These parameters depend upon the physical system we choose to discuss: for the optical processes, either the coupled cavities or the propagation of two electromagnetic field modes in interferometers with a Kerr medium, they are related to the third-order nonlinear susceptibility $\chi^{(3)}$ [9, 10], and for the two interacting BEC species, they are functions of the s-wave scattering length a_{ij} [11]. In this context, the Hamiltonian above is obtained from the multi-mode second quantized Hamiltonian, in the two-mode approximation, which consists in neglecting all modes except the condensate ones, as described, for example, in Gordon and Savage [18, 11].

Since our purpose here is to have an exactly solvable model with the nonlinearities in such a way that we could see the effect of each interaction term on the entanglement dynamics, we shall just set $g_{12} = g_1 = g_2 = g$ and also choose the resonant case[2] ($\omega_1 = \omega_2$) with $\omega_0 = \omega_k + \hbar g$ such that the Hamiltonian can be rewritten in the following form:

$$\begin{aligned}\hat{H} &= \hbar\omega_0\sum_{k=1}^{2}\left[\left(\hat{a}_k^\dagger\hat{a}_k + \frac{1}{2}\right)\right] + \hbar\lambda\left(\hat{a}_1^\dagger\hat{a}_2 + \hat{a}_1\hat{a}_2^\dagger\right) + \hbar^2 g\left(\hat{a}_1^\dagger\hat{a}_1 + \hat{a}_2^\dagger\hat{a}_2 + 1\right)^2 \\ &= \hat{H}_0 + \hat{V}_\lambda + \hat{V}_g.\end{aligned} \tag{2}$$

Note that the entire nonlinear interaction, $\hat{V}_g$, is now in the form of the square of the free Hamiltonian $\hat{H}_0$, and hence the following commutation relations hold:

$$[\hat{H}_0, \hat{V}_\lambda] = [\hat{V}_g, \hat{V}_\lambda] = 0. \tag{3}$$

This property allows us to study separately the action of each interaction term present in the evolution operator on the initial state, and hence, examine its consequences on the entanglement process. In what follows, our aim is to solve the Schrödinger equation exactly for specific initially separable conditions

$$|\psi(t)\rangle = \mathrm{e}^{-\frac{\mathrm{i}}{\hbar}\hat{H}t}|\psi(0)\rangle = \mathrm{e}^{-\frac{\mathrm{i}}{\hbar}\hat{H}t}|\psi_1(0)\rangle \otimes |\psi_2(0)\rangle \tag{4}$$

and study the evolution of initially uncorrelated Fock and coherent states. The former state is generally studied in connection with Bose–Einstein condensates, whereas the latter is for the nonlinear optical system.

[2] We note that this choice, in both applications mentioned above, is qualitatively plausible. In the case of nonlinear media, since the frequencies of the two propagating modes are the same, the self-modulation terms must also be present (see [9]), and the adiabatic condition [29] is preserved. As for the BECs, the restricted solution corresponds to equal s-wave scattering lengths for all collisions ($a_{11} = a_{22} = a_{12}$) (see [11]), and the new choice is close to the experimental situation (see [25]).

2.1. Analytical solutions for a product of coherent states

We consider first the case of initially disentangled Fock states, in order to establish notation

$$|\psi(0)\rangle = |n_1\rangle \otimes |n_2\rangle\,. \tag{5}$$

We have used the canonical transformation proposed by Zoubi *et al* [27] that preserves the total excitation number, $\hat{N}$, which is a constant of motion of the general Hamiltonian (1): $\hat{a}_1^\dagger \hat{a}_1 + \hat{a}_2^\dagger \hat{a}_2 \equiv \hat{N}$. This number could correspond either to the total particle number of the two interacting BECs or the total number of photons associated with the field modes interacting in a Kerr medium. It is straightforward to obtain a diagonalized Hamiltonian as follows:

$$\hat{H} = \hbar\,(\omega_0 + \lambda)\left(\hat{N}_1 + \tfrac{1}{2}\right) + \hbar\,(\omega_0 - \lambda)\left(\hat{N}_2 + \tfrac{1}{2}\right) + \hbar^2 g(\hat{N}_1 + \hat{N}_2 + 1)^2. \tag{6}$$

The time-evolved state is then given by

$$\begin{aligned} |\psi(t)\rangle &= \mathrm{e}^{-\mathrm{i}\Phi}\hat{\Gamma}_{12}^{(n_1)}(t)\hat{\Gamma}_{21}^{(n_2)}(t)|0,0\rangle \\ \hat{\Gamma}_{kk'}^{(n)}(t) &\equiv \frac{\left(\hat{a}_k^\dagger \cos\lambda t - \mathrm{i}\hat{a}_{k'}^\dagger \sin\lambda t\right)^n}{\sqrt{n!}}. \end{aligned} \tag{7}$$

The sub-indices '12' ('21') of the operators $\hat{\Gamma}$ emphasize the entanglement features of the dynamics, and the global phase is given by $\Phi = [\omega_0 t\,(N+1) + \lambda t N + \hbar g t\,(N+1)^2]$. Note that this solution coincides with the one which describes a linear beam splitter [28].

Now, we can extract information about the entanglement process of Fock states under the action solely of the bilinear interaction. From equation (7) one can extract two periods where the system is in a disentangled state:

(i) *purification times* $T_l = \frac{\pi}{\lambda}(l + \frac{1}{2})$, where the subsystems are disentangled, but not in the same states as the initial one.
(ii) *recurrence times* $\tau_l = l\frac{\pi}{\lambda}$, where the system returns to the exact initial state (modulo an overall phase).

In the context of BEC, this situation corresponds to a separable initial state with n_1 bosons in mode 1 and $N - n_1$ in the other mode, for which after an interval of time corresponding to $\lambda t = \pi/2$, we expect an exchange in the occupation numbers. In the optical schemes, this property indicates that RWA-coupling leads the initial state to a new separable one, but with the number of photons exchanged. This allows us to classify $|\psi(0)\rangle$ in equation (5) as a *reversible state* for this bilinear interaction. As a consequence, we can define a *period of reversibility* for such states: $\tau_R = \frac{\pi}{\lambda}$. For the special case of initial Fock states with equal numbers ($n_1 = n_2 = N/2$), the difference between the purification and recurrence times disappears and the reversibility occurs earlier.

The above solution can be used to analyse the temporal evolution of any initial state written as a superposition of Fock states. A special type of state of interest in the case of Josephson coupled BECs in a two-mode approximation, is the case where (due to the conservation of the number of particles) a general state can be written as follows [15]:

$$|\psi\rangle_{\mathrm{BEC}} = \sum_{n=0}^{N} c_n |n\rangle |N-n\rangle \tag{8}$$

where n and $N - n$ are the populations in each mode and c_n are complex numbers.

In what follows, we present the solution of the Schrödinger equation, equation (4), when the initial state is a direct product of coherent states. Our interest in this case, mainly focused on the optical systems, is twofold: the possibility of studying the formation of a superposition of coherent states in one of the subsystem phase spaces; and the possibility of analysing how

the dynamics of entanglement changes when the classical action associated with the mean number of photons becomes larger than the Planck constant.

Consider an initially disentangled product of two coherent states as follows:

$$|\psi(0)\rangle = |\alpha_1\rangle \otimes |\alpha_2\rangle \, \mathrm{e}^{\frac{-|\alpha_1|^2}{2}} \, \mathrm{e}^{\frac{-|\alpha_2|^2}{2}} \sum_{n,m} \frac{\alpha_1^n}{\sqrt{n!}} \frac{\alpha_2^m}{\sqrt{m!}} |n, m\rangle. \tag{9}$$

In the optical context, such a state is the most common one to be generated in the laboratory, either in the interferometers or in the cavities, whereas, to the authors' knowledge, such a state has not been generated corroboratively in the case of BECs.

The time-evolved state can be obtained using the previous result, equation (7),

$$|\psi(t)\rangle = \mathrm{e}^{\frac{-|\alpha_1|^2-|\alpha_2|^2}{2}} \sum_{n,m} \frac{\alpha_1^n(t)}{\sqrt{n!}} \frac{\alpha_2^m(t)}{\sqrt{m!}} \mathrm{e}^{-\mathrm{i}\hbar g(n+m+1)^2 t} \Gamma_{12}^{(n)}(t) \Gamma_{21}^{(m)}(t) |0, 0\rangle \tag{10}$$

where $\alpha_k(t) = \alpha_k \, \mathrm{e}^{-\mathrm{i}(\omega_0+2\hbar g)t}$. In this result we have already omitted a global phase.

It is easy to see, for $g = 0$, that the bilinear coupling does not entangle the modes, since the two summations of equation (10) can be factorized, and each subsystem remains in a coherent form

$$\begin{aligned} |\psi(t)\rangle|_{g=0} &= \hat{D}_1[\beta_1(t)]\hat{D}_2[\beta_2(t)]|0, 0\rangle \\ &= |\beta_1(t), \beta_2(t)\rangle \end{aligned} \tag{11}$$

where $\hat{D}_k[\beta_k(t)] = \mathrm{e}^{(\beta_k \hat{a}_k^\dagger - \beta_k^* \hat{a}_k)}$ is the coherent state displacement operator in the phase space of the kth oscillator and

$$\beta_{\substack{1\\2}}(t) = \left(\alpha_{\substack{1\\2}} \mathrm{e}^{-\mathrm{i}\omega_0 t} \cos \lambda t - \mathrm{i}\alpha_{\substack{2\\1}} \mathrm{e}^{-\mathrm{i}\omega_0 t} \sin \lambda t\right). \tag{12}$$

Using this particular result, we can solve the general case of initially disentangled coherent states in a more intuitive way. The commutation relations (3) allow us to apply separately the piece of the evolution operator associated with the nonlinear term of $\hat{H}$, equation (2), and use the previously derived results (equations (10, 11)). The final exact solution for the temporal evolution of two initially coherent states is given by

$$\begin{aligned} |\psi(t)\rangle &= \mathrm{e}^{\frac{gt\hat{H}_0^2}{\mathrm{i}\hbar}} \mathrm{e}^{\frac{\omega t\hat{H}_0+\lambda t\hat{V}}{\mathrm{i}\hbar}} |\alpha_1, \alpha_2\rangle \\ &= \mathrm{e}^{\frac{gt\hat{H}_0^2}{\mathrm{i}\hbar}} |\beta_1(t), \beta_2(t)\rangle \\ &= \mathrm{e}^{-\frac{|\alpha_1|^2+|\alpha_2|^2}{2}} \sum_{n,m} \mathrm{e}^{-\mathrm{i}\hbar gt(n+m)^2} \frac{[\beta_1(t)\mathrm{e}^{-\mathrm{i}2g\hbar t}]^n}{\sqrt{n!}} \frac{[\beta_2(t)\mathrm{e}^{-\mathrm{i}2g\hbar t}]^m}{\sqrt{m!}} |n, m\rangle \, . \end{aligned} \tag{13}$$

Here, the expressions of $\beta_k(t)$ are those depicted in equation (12).

In order to calculate other quantities such as the mean values and variances of the quadrature operators, let us obtain the density operator of the system. Since we are interested in the case where the global system is isolated, the total density operator is a projector onto the state $|\psi(t)\rangle$

$$\begin{aligned} \hat{\rho}(t) &= |\psi(t)\rangle\langle\psi(t)| \\ &= \mathrm{e}^{-\frac{\Lambda}{2\hbar}} \sum_{n,m} \sum_{n',m'} \mathrm{e}^{-\mathrm{i}\hbar gt[(n+m+1)^2-(n'+m'+1)^2]} \frac{\beta_1^n \beta_1^{*n'} \beta_2^m \beta_2^{*m'}}{\sqrt{n!n'!m!m'!}} |n, m\rangle\langle n', m'| \end{aligned} \tag{14}$$

where we have defined $\Lambda = |\alpha_1|^2 + |\alpha_2|^2$, a characteristic action of the system. We shall denote from here on $\beta_k(t)$ simply as β_k. We calculated the reduced density operators $\hat{\rho}_k(t)$ $(k = 1, 2)$

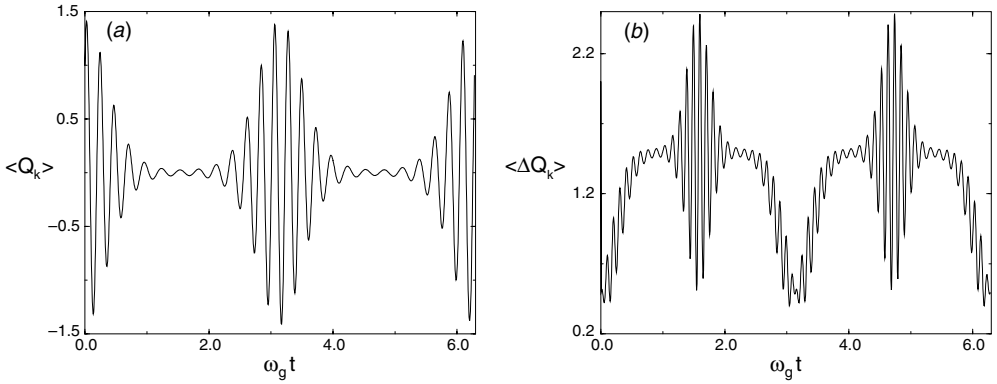

Figure 1. (*a*) Collapse and revival phenomena in the evolution of the expectation value of the quadrature $\hat{Q}_k$ and (*b*) the respective variance. Analytical results for $\frac{\omega_0}{\omega_g} = 20$, $\frac{\lambda}{\omega_g} = 2$, $q_{k0} = p_{k0} = 1.0$, $\Lambda = 4.0$ and $\hbar = 1$. The same qualitative behaviour is observed for $\langle \hat{P}_k \rangle(t)$ and $\langle \Delta \hat{P}_k \rangle(t)$.

by tracing over the undesired degree of freedom, corresponding to one of the original bosonic modes:

$$\hat{\rho}_1(t) = \mathrm{e}^{-\frac{\Lambda}{2\hbar}} \sum_{n,m} \frac{\beta_1^n}{\sqrt{n!}} \frac{\beta_1^{*m}}{\sqrt{m!}} \mathrm{e}^{|\beta_2|^2 \mathrm{e}^{-2\mathrm{i}\hbar g t(n-m)}} \mathrm{e}^{-\mathrm{i}\hbar g t[n^2-m^2+2(n-m)]} |n\rangle\langle m| \tag{15}$$

with a similar expression for $\hat{\rho}_2(t)$. The field quadrature operators $\hat{Q}_k$ and $\hat{P}_k$ are given in terms of the creation and annihilation operators as follows:

$$\begin{pmatrix} \hat{Q}_k \\ \hat{P}_k \end{pmatrix} = \sqrt{\frac{\hbar}{2}} \begin{bmatrix} 1 & 1 \\ -\mathrm{i} & \mathrm{i} \end{bmatrix} \begin{pmatrix} \hat{a}_k \\ \hat{a}_k^\dagger \end{pmatrix} \tag{16}$$

and analytical expressions for the mean values are given by

$$\begin{aligned} \langle \hat{Q}_k \rangle(t) &= \mathrm{Tr}_k[\hat{Q}_k \hat{\rho}_k(t)] \\ &= \sqrt{2\hbar}\, \mathrm{Re}[\beta_k(t)\, \mathrm{e}^{-3\mathrm{i}\omega_g t}\, \mathrm{e}^{-\frac{\Lambda}{2\hbar}(1-\mathrm{e}^{-2\mathrm{i}\omega_g t})}] \end{aligned} \tag{17}$$

$$\begin{aligned} \langle \hat{P}_k \rangle(t) &= \mathrm{Tr}_k[\hat{P}_k \hat{\rho}_k(t)] \\ &= \sqrt{2\hbar}\, \mathrm{Im}[\beta_k(t)\, \mathrm{e}^{-3\mathrm{i}\omega_g t}\, \mathrm{e}^{-\frac{\Lambda}{2\hbar}(1-\mathrm{e}^{-2\mathrm{i}\omega_g t})}] \end{aligned} \tag{18}$$

where we defined the frequency associated with the nonlinear term as $\omega_g = \hbar g$.

The above expressions contain exponentials of oscillatory terms, which produce the *collapse* and *revival* phenomena [29] at times that are odd multiples of $\frac{\pi}{2\omega_g}$ and integer multiples of $\frac{\pi}{\omega_g}$ respectively, as shown in figure 1(*a*) where we plotted the mean value of $\hat{Q}_k$ quadrature as a function of $\omega_g t$.

One can also calculate analytically the *variances* $\langle \Delta Q_k \rangle(t)$ and $\langle \Delta P_k \rangle(t)$. The results are complicated expressions which we shall omit. However, the general behaviour is presented in figure 1(*b*), where we can see the same periodic structure present in the quadrature mean value temporal behaviour. These results for the subsystem variances are very similar to those obtained for the one degree of freedom quartic oscillator [19]. The most instructive information is the relation between the collapse and the phase space's *delocalization in phase* of the state, as can be seen in the projected Q-function that will be illustrated in the next section for a particular set of parameters.

3. Entanglement properties and their semiclassical behaviour

In this section, we are going to discuss the entanglement dynamics of time-evolved states found in section 2; namely, the product of Fock states and coherent states. We analyse the subsystem entropy, one important tool that gives a measure of entanglement for globally pure bipartite systems. In the second case, we also use the Husimi distribution or Q-function, in order to follow the evolution of the partial distribution in phase space. The Q-function for the global system is usually defined by

$$Q(\vec{q}, \vec{p}) = \frac{1}{\pi}\langle\gamma_1\gamma_2|\hat{\rho}(t)|\gamma_1\gamma_2\rangle \tag{19}$$

where we choose $\gamma_k = \frac{q_k + \mathrm{i}p_k}{\sqrt{2\hbar}}$ $(k = 1, 2)$. In particular, we investigate the role played by the nonlinear interaction term in the Hamiltonian (2) which appears associated with the frequency ω_g in the various analytical expressions derived. Moreover, we would like to find the behaviour of the subsystem linear entropies in the *semiclassical limit*.

3.1. Entanglement properties of Fock states

For this initial state, we are interested in the calculation of both the subsystem von Neumann entropy (SVNE) and the subsystem linear entropy (SLE), usually defined by

$$S_k = -\mathrm{Tr}_k(\hat{\rho}_k \ln \hat{\rho}_k) \qquad \delta_k = 1 - \mathrm{Tr}_k\left(\hat{\rho}_k^2\right) \tag{20}$$

where the label k is associated with one of the degrees of freedom. In terms of the reduced density operator eigenvalues, both entropies assume the familiar form:

$$S_k(t) = -\sum_{l=0}^{N} \lambda_l(t) \ln(\lambda_l(t)) \qquad \delta_k(t) = 1 - \sum_{l=0}^{N} \lambda_l(t)^2. \tag{21}$$

For the initially disentangled Fock states, equation (5), the reduced density operator is diagonal; therefore, it can be directly expressed in terms of its eigenvalues as follows:

$$\rho_k(t) = \sum_{l=0}^{N} \lambda_l(t)|l\rangle\langle l| \tag{22}$$

and the trace condition $\sum \lambda_l(t) = 1$ must be satisfied. The eigenvalues $\lambda_l(t)$ are given by

$$\lambda_l(t) = \sum_{i,i'=0}^{n_1} \sum_{m,m'=0}^{N-n_1} c_{i,m}(t) c^*_{i',m'}(t) \delta_{i-m,i'-m'} \delta_{n_1-l,i-m} \tag{23}$$

$$c_{i,m}(t) = \binom{n_1}{i}\binom{N-n_1}{m}\sqrt{\frac{(n_1 - i + m)!(n_1 - m + i)!}{n_1!(N - n_1!)}}(\cos\lambda t)^{N-(i+m)}(-\mathrm{i}\sin\lambda t)^{i+m}. \tag{24}$$

The dependence of the eigenvalues on the periodic functions confirms the conditions for the purification times as we already noted from the time-evolved state equation (7). To illustrate what has been discussed above, we present some simple examples:

- For $|\psi(0)\rangle = |1, 0\rangle$ we have

$$\begin{cases} \delta_k(t) = \frac{1}{2}\sin^2 2\lambda t \\ S_k(t) = -\cos^2\lambda t \ln(\cos^2\lambda t) - \sin^2\lambda t \ln(\sin^2\lambda t). \end{cases} \tag{25}$$

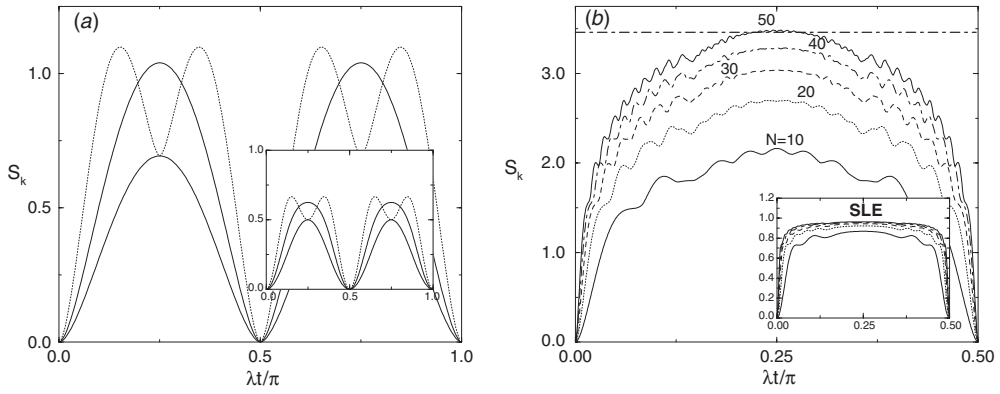

Figure 2. (*a*) Von Neumann entropy for three different sets of initial two Fock states: $|1, 0\rangle$ (solid line), $|1, 1\rangle$ (dashed line) and $|2, 0\rangle$ (solid thick line). Inset: linear entropy for the same cases. (*b*) Von Neumann entropy for the initial state $(|n_1, N - n_1\rangle)$, with $n_1 = 0.8N$ and several values of N and the dashed line is the maximum possible entanglement value for $N = 10$. Inset: linear entropy for the same values of N.

- For $|\psi(0)\rangle = |1, 1\rangle$ we have

$$\begin{cases} \delta_k(t) = \frac{\sin^2 2\lambda t}{4}\,(5 + 3\cos 4\lambda t) \\ S_k(t) = -\cos^2 2\lambda t \ln(\cos^2 2\lambda t) - \sin^2 2\lambda t \ln\left(\frac{\sin^2 2\lambda t}{2}\right). \end{cases} \tag{26}$$

- For $|\psi(0)\rangle = |2, 0\rangle$ we have

$$\begin{cases} \delta_k(t) = \frac{\sin^2 2\lambda t}{16}\,(13 + 3\cos 4\lambda t) \\ S_k(t) = -\cos^4 \lambda t \ln(\cos^4 \lambda t) - \sin^4 \lambda t \ln(\sin^4 \lambda t) \\ -\frac{\sin^2 2\lambda t}{2} \ln\left(\frac{\sin^2 2\lambda t}{2}\right). \end{cases} \tag{27}$$

A comparison of analytical results for both SVNE and SLE are shown in figure 2. We see both quantities predict the same purification times, when both entropies are zero. Also, the general behaviour is the same and the analysis of the entanglement process can be performed without loss of information. Only in the cases where the number of participating basis states (in one or both subsystems) becomes very large, do the details near the values close to the maximum value of the SLE (close to one) become squeezed. So, we have chosen to work with SVNE whenever this is the case, otherwise we will plot the SLE due to the simplicity of its calculation. Comparing our results in figure 2(*a*), it is interesting to observe that the general behaviour is similar for cases $|1, 0\rangle$ and $|2, 0\rangle$, and different for $|1, 1\rangle$. The maximum value of entanglement depends on the value of N, but the general behaviour is not the same for initial states with the same N. In fact, local maxima and minima structure are sensitive to the difference between occupation numbers. This is better illustrated in figure 2(*b*) where von Neumann entropy is plotted for several values of N, and choosing $n_1 = 0.8N$ and $N - n_1 = 0.2N$. We can see how both the maximum value of entanglement reached for each curve and the number of oscillations increase as N increases. This feature can be understood from equation (22), where the number of accessible states is given by $N + 1$ which increases with increasing total number of excitations, N. This accounts for the increase in the maximum value of entropy, and also the subsystem is allowed to pass through many more possible states, although this maximum does not correspond to the maximally entangled state allowed for this system (much higher than the value actually attained as indicated by the dashed line in the

case $N = 10$). However, one can see clearly that as long as we choose the same proportion for the initial populations of Fock states of different modes, the general behaviour is the same as we increase the total number of excitations N. The times at which the maximum value is reached is the same for all cases, and the oscillatory structure is also similar.

Note that no dependence on $\hbar$ or g is essentially left in the expression of the time-evolved state (7), and the same happens for the calculated reduced density eigenvalues (equations (23) and (24)). This is the case where the nonlinear interaction plays no role, and the semiclassical limit is related to the presence of many particles (atoms or photons), namely large N. We can predict the behaviour of entanglement in this limit: as N increases, the subsystems entangle faster, and the maximum value of von Neumann entropy increases, although its value for maximally entangled states also increases proportionally with N.

3.2. Entanglement properties for coherent states

In order to study the entanglement dynamics and reversibility properties for the initial product of coherent states, we calculate the SLE defined in equation (20). Using our result for the subsystem density operator, equation (14), an exact expression for this quantity can be calculated:

$$\begin{aligned}\delta_1(t) &= 1 - \mathrm{Tr}_1\left(\hat{\rho}_1^2(t)\right) \\ &= 1 - \mathrm{e}^{-2|\beta_1(t)|^2} \sum_{n,m} \frac{|\beta_1(t)|^{2n}}{n!} \frac{|\beta_1(t)|^{2m}}{m!} \mathrm{e}^{-4|\beta_2(t)|^2 \sin^2[\hbar g t(n-m)]}. \end{aligned} \tag{28}$$

In a similar fashion as in the case of the Fock states, we can find the purification times by studying the conditions under which $\delta_1(t)$ is equal to zero, indicating that the subsystems are disentangled. A simple analysis of equation (28) shows that this happens in the following situations:

(i) For any initial conditions excluding the vacuum state ($|0, 0\rangle$), the purification times associated with the nonlinear interaction are $\hbar g T_l = l\pi$, when the argument of the sine-function is an integer multiple of π:

$$T_l = l\frac{\pi}{\hbar g} \qquad (l > 0 \text{ integer}). \tag{29}$$

At these times, the system state evolves from the initial state to a new product of coherent states given by

$$|\psi(T_l)\rangle = |(-1)^l \beta_1(T_l)\rangle \otimes |(-1)^l \beta_2(T_l)\rangle. \tag{30}$$

(ii) For those initial conditions such that one of the arguments $\beta_k(t) = 0$, one can find other instances when SLE is zero. These conditions are associated exclusively with bilinear coupling and special initial conditions. In terms of the quadratures of the initial values α_k, and using expression (12) one can write these conditions as follows:

$$q_1 q_2 + p_1 p_2 = 0$$

and we have disentangled states for times:

$$t_1 = \frac{1}{\lambda}\arctan\left(-\tfrac{q_1}{p_2}\right) \qquad \text{or} \qquad t_2 = \frac{1}{\lambda}\arctan\left(\tfrac{p_1}{q_2}\right).$$

If we evaluate equation (14) at this time, considering $\beta_2 = 0$ and $\beta_1 \neq 0$, we obtain a direct product formed by subsystem one in a state written as (remembering that β_1 depends on time)

$$|\psi_1(t_1)\rangle = \mathrm{e}^{-\frac{|\beta_1|^2}{2}} \sum_n \mathrm{e}^{-\mathrm{i}\omega_g t_1 n^2} \frac{[\beta_1 \mathrm{e}^{-\mathrm{i}2\omega_g t_1}]^n}{\sqrt{n!}} |n\rangle \tag{31}$$

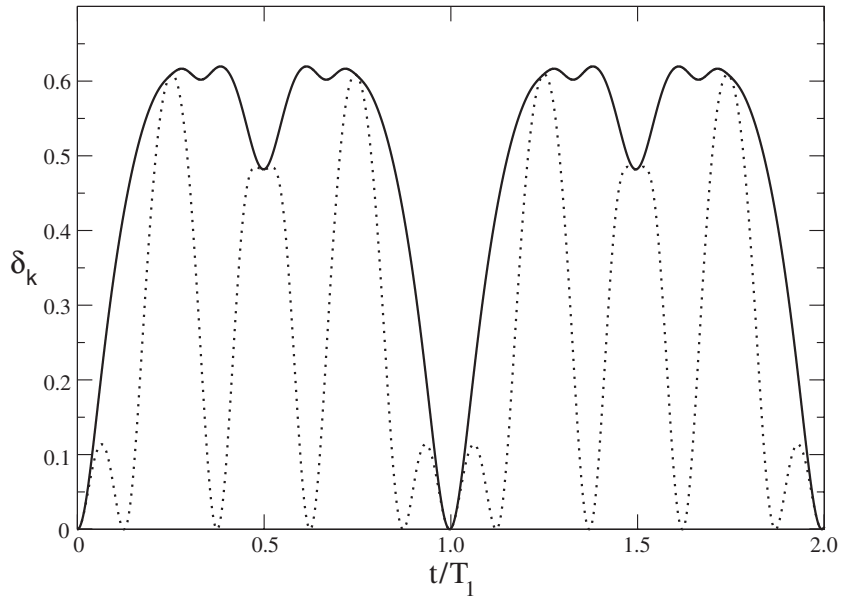

Figure 3. SLE as a function of dimensionless parameter t/T_1 for an initial state as a direct product of coherent states. Here $T_1 = \frac{\pi}{\hbar g}$ is a first purification time, $\hbar = 1.0$, $g = 0.1$, $\lambda = 0.2$ and $\omega_0 = 1.0$. Solid line: $q_{01} = p_{01} = q_{02} = p_{02} = 1.0$. Dotted line: $q_{01} = 1.0$, $p_{01} = 1.0$, $q_{02} = -p_{01}$ and $p_{02} = q_{01}$, satisfying the second condition.

and subsystem two in the vacuum state. If $\hbar g t_1 = \frac{r}{s}$, with r and s integers, we can rewrite the expression as a *superposition of coherent states*, as we see in the appendix.

Among these purification times, we can identify those at which we also have recurrences by examining equation (14). Only the first class of conditions produces recurrences, and this happens *for a given value of T_l, when the ratios $l\frac{\omega_0}{\omega_g}$ and $l\frac{\lambda}{\omega_g}$ are integer numbers*.

To illustrate the dynamics of entanglement in these two cases, we present in figure 3 the results for the subsystem linear entropy as a function of dimensionless parameter t/T_1, with $T_l = l\pi/\omega_g$. We choose two initial α_k values: in the first case (solid line), SLE only possesses null values for times corresponding to case (i). At times different from the T_l, the value of SLE is different from zero indicating that the subsystems are entangled. The situation changes when initial $\alpha_{1,2}$ are chosen such that condition (ii) is verified (dotted line). For this case, we obtain times different from T_l where SLE is null. For a particular choice of parameters shown in figure 3, $\lambda t_k^j = \pm 1$ and we can define a new purification period as follows:

$$T_l' = l\frac{\pi}{4\lambda} \tag{32}$$

where l is an *odd* integer. As we already noted before, at these times Schrödinger cat states are dynamically generated (times $\frac{T_l'}{T_1} = 0.2, 0.4, 0.6, 0.8$ in figure 3).

We also note that another class of initially disentangled states that can be solved exactly is that of the form $|\alpha_1\rangle \otimes |n_2\rangle$. For such a class, the type of analysis presented above also works, and one can find purification times such that one of the subsystems becomes a superposition of coherent states [30].

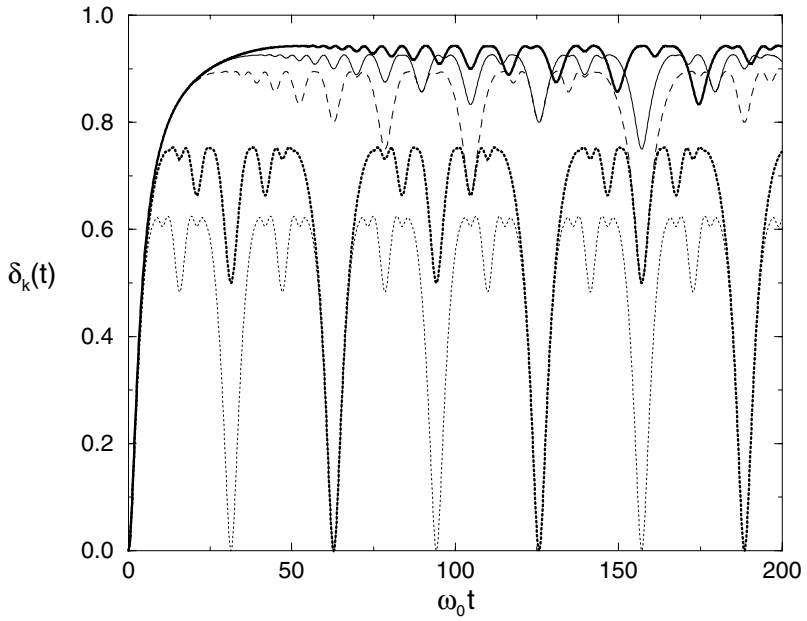

Figure 4. Subsystem linear entropy δ_k as a function of $\omega_0 t$ for $\frac{\lambda}{\omega_0} = 0.2$, $\frac{\omega_g}{\omega_0} = 0.1$, $q_{k0} = p_{k0} = 1.0$, $\Lambda = 4$ and several values of $\mathcal{R} = \frac{\hbar}{\Lambda}$: $\mathcal{R} = \frac{1}{4}$ (dotted line), $\mathcal{R} = \frac{1}{8}$ (dotted thick line), $\mathcal{R} = \frac{1}{40}$ (dashed line), $\mathcal{R} = \frac{1}{80}$ (solid line) and $\mathcal{R} = \frac{3}{400}$ (solid thick line).

3.3. Semiclassical behaviour and break time

Now we will choose particular parameter sets to illustrate the semiclassical limit of the SLE, since in contrast to the case of the product of Fock states, we have an explicit dependence on $\hbar$, actually on the frequency $\omega_g = \hbar g$. This allows us to study the semiclassical behaviour of the SLE. The natural parameter to measure the 'quantumness' of the system here is the ratio $\mathcal{R} = \frac{\hbar}{\Lambda}$, where Λ (defined in section 2.1) is a characteristic action in phase space. In figure 4 we plotted the time evolution of the SLE for several values of $\mathcal{R}$. Here, we adopted the convention to fix the value of Λ and vary $\hbar$ instead in the opposite way. The first thing to be noted is the fact that all curves coincide at the short time scale, where the SLE increases monotonically until it reaches the maximum value. The maximum value of SLE depends on $\mathcal{R}$, which increases as we let $\mathcal{R} \ll 1$. This has to do with the increasing number of accessible states as we let the spectrum become denser, and also implies loss of information. We will call this first regime the '*phase spread regime*' in connection with the behaviour of the Q-function of each subsystem that we shall see in what follows. After reaching the maximum value, oscillations start in the SLE, which can be seen as a partial recovery of coherence, until the first purification time $T_1 = \frac{\pi}{g\hbar}$ (see equation (29)) at which $\delta_k = 0$ and the subsystem recovers purity. This second regime will be called '*self-interference regime*' since the time-evolved subsystem Q-function shows the phenomenon of self-interference typical of the Kerr-type nonlinearity. This is consistent with the fact that in the limit $\mathcal{R} \to 0$ the purification time goes to infinity and the initial purity will never be recovered. We will call *break time* t_b, the time at which the transition from the phase spread regime (rising) to the self-interference (oscillating) regime occurs. It is clear from figure 4 that this time increases with the inverse power of $\mathcal{R}$, and we also expect it to go to infinity in the classical limit.

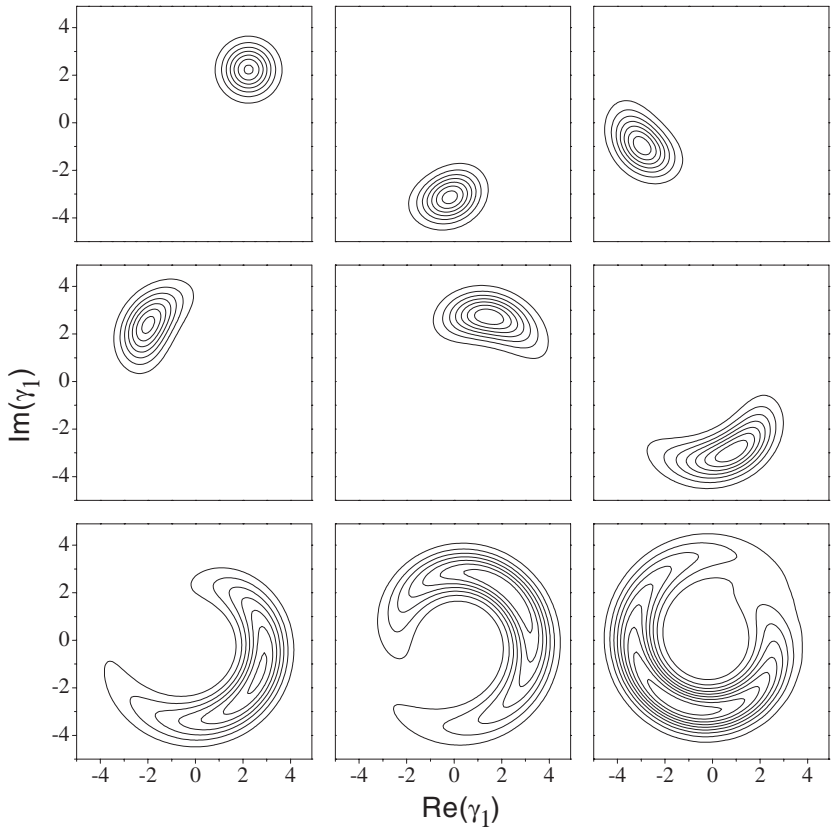

Figure 5. Contour plot of subsystem Q-function in the plane (q_1, p_1) during the *phase spread regime*, for initial conditions $q_{10} = p_{10} = q_{20} = p_{20} = 1.0, \omega_0 = 1, \lambda = 0.2, g = 0.1$ and $\mathcal{R} = 0.025$. The first plot corresponds to the initial time (upper-left corner) and the subsequent times are chosen in the interval $0 < t \leqslant t_b$.

Let us illustrate the differences between the two regimes by means of the subsystem Q-function which will show the proper signatures in each regime. In figure 5 we plotted Q-function in various instances of the *phase spread regime* for the same Hamiltonian parameters used in figure 4, and the quantumness parameter $\mathcal{R} = 0.025$. The sequence of plots is in the quadrature plane of the mode-1, beginning at $t = 0$ until $t \approx t_b$. In this case the centre of the initially coherent Gaussian wave-packet follows essentially the classical trajectory, as predicted by the Ehrenfest theorem [31], circulating around the origin and, due to the nature of the self-interaction term, the packet itself spreads in phase angle in the phase space. During the interval of time before the front of the packet reaches its tail [19] no purifications can happen.

In figure 6, another sequence of contour plots of Q-functions of the subsystem-1 shows a time evolution during the *self-interference regime* in the interval of time after the break time t_b, until the first purification time T_1. We also add a plot at the recurrence time ($\tau_1 = 2T_1$ for this particular set of parameters). The appearance of several peaks along the annular region is remarkable, a signature of self-interference phenomenon where a kind of standing wave with M-peaks forms at times $t = T_1/M$ (for $t > t_b$), when the SLE assumes the value $\delta_k \approx 1 - \frac{1}{M}$ at a local minimum. This kind of behaviour is a hallmark of the self-interference

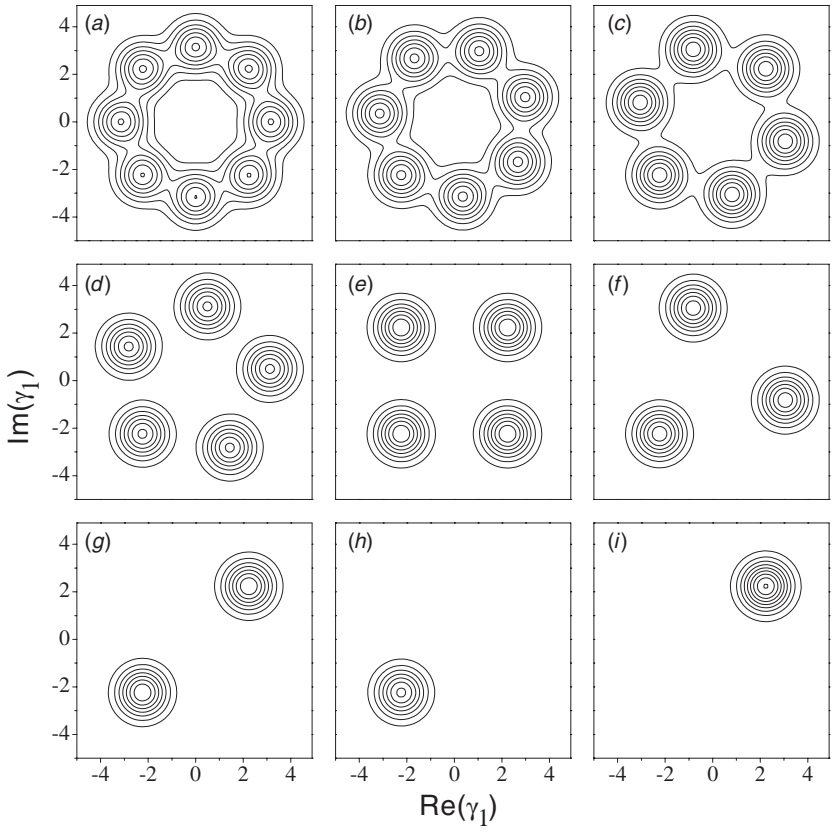

Figure 6. Time evolution of contour plots of a subsystem Q-function during the *self-interference regime* for $\mathcal{R} = 0.025$ in the plane (q_1, p_1), with the same parameter values of figure 5. (*a*) $t = T_1/8$, (*b*) $t = T_1/7$, (*c*) $t = T_1/6$, (*d*) $t = T_1/5$, (*e*) $t = T_1/4$, (*f*) $t = T_1/3$, (*g*) $t = T_1/2$, (*h*) $t = T_1$ (first purification time), (*i*) $t = 2T_1 = \tau_1$ (recurrence).

regime, an essentially quantum phenomenon which is at the core of purification possibilities and reversibility in this system.

At first sight, one could think that the break time would have the same dependence on the Planck constant as T_1, but this is not true. In fact, the actual relation between break time and $\mathcal{R}$ parameter is given by

$$t_b \approx \frac{1}{\Lambda g}\sqrt{\frac{\Lambda}{\hbar}}.$$

This relation shows that our t_b is the *same* as the Ehrenfest scale calculated for a nonlinear quartic oscillator by Berman *et al* [32]. Also, the Planck constant and characteristic action dependence coincide with the results obtained in [33, 34] for the present model in the case $\lambda = 0$.

4. Comments on a realistic parameter regime

Since our analytical solution is restricted to the case $g_1 = g_2 = g_{12}$, we show here some numerical evidence indicating that, even in a more realistic case where such a condition is

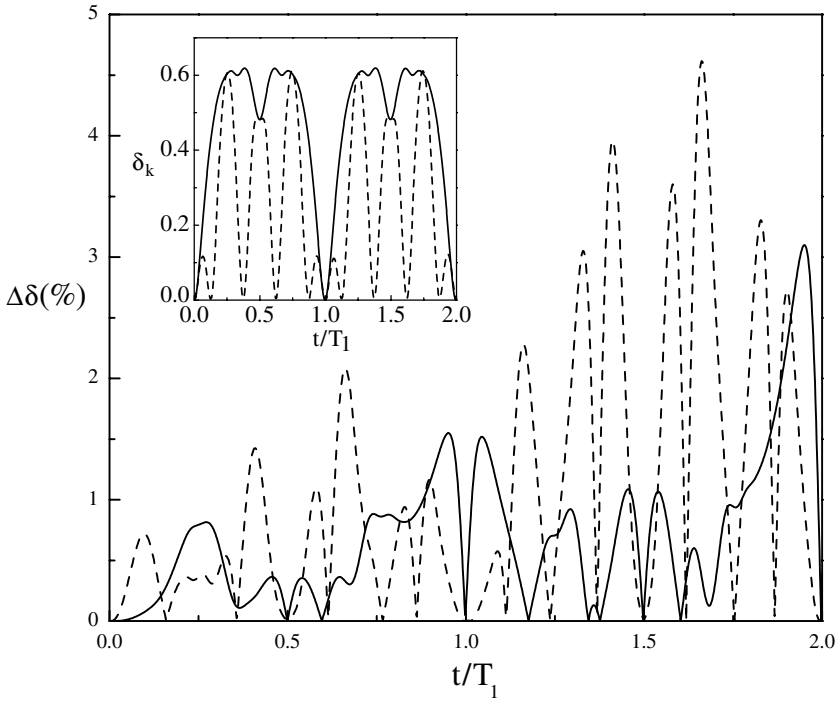

Figure 7. Comparison of the numerical results for the subsystem linear entropy obtained with $(g_1{:}g_2{:}g_{12}) = (1.03{:}0.97{:}1)$ and the exact case of figure 3 (with the same initial conditions and corresponding line conventions): percentage of the difference between the exact case and this specific choice with respect to the maximal value of SLE as a function of dimensionless time t/T_1. Inset: time evolution for the SLE.

not fulfilled, most of our results are at least qualitatively preserved. In order to see that this is indeed the case, let us consider the following values for the coupling parameters: $g_1{:}g_2{:}g_{12} = 1.03{:}0.97{:}1$. As for the BECs, the restricted solution corresponds to equal s-wave scattering lengths for all collisions ($a_{11} = a_{22} = a_{12}$) (see [11]), and the new choice is close to the experimental situation (see [25]). In order to obtain numerically the reduced linear entropy, we have diagonalized the Hamiltonian (2) using a harmonic oscillator basis of size $n_{1\max} = n_{2\max} = 50$, and calculated the time evolution of the initial state (9) with the same values of q_i, p_i used in figure 3. The time-evolved density operator $|\psi(t)\rangle\langle\psi(t)|$ is then obtained in the harmonic oscillator basis, and the partial trace is taken on one of the basis indices $n_{1,2}$ to get the reduced density operator $\hat{\rho}_{2,1}(t)$. The numerical reduced linear entropy obtained in this way is plotted in figure 7, where $\Delta\delta$ is the percentage of the difference between our exact solution ($g_1 = g_2 = g_{12}$) and numerical results for the choice above mentioned with respect to the maximal value of entropy, for both initial states of figure 3. Both percentages are smaller than 5%, hence the general behaviour of the reduced linear entropy is quite similar to the analytical case, as can be seen in the inset. It is remarkable that, at those purification times related only to the nonlinear interaction $\Delta\delta$ is null, whereas at those associated with initial conditions (times of cat state formation) this quantity is not exactly zero, but small (lower than 0.1%). These results suggest that even in the realistic case, where the condition of equal couplings is not satisfied, the physics should not change very much as compared with the one presented in the previous section.

5. Conclusions

We have solved analytically a problem of two resonant bilinearly interacting bosonic modes in the presence of nonlinear (quartic or two-body) interactions. The time-evolved state has been exactly determined in the case of initially separable states, for both Fock states and coherent states. This allowed us to study the entanglement dynamics of the two bosonic modes, either in the scenario of two interacting BECs or two electromagnetic field modes. The reduced density operator has been obtained analytically, and this allowed us to discuss several properties of entanglement between the two modes for both initial conditions.

For the initial state corresponding to a separable product of *Fock states*, the bosonic modes could be associated with an idealized system of two species of BECs with well-defined occupation numbers in the two-mode approximation. We have shown that the Josephson-type coupling (bilinear) naturally leads the total system to an entangled state with other possible occupation numbers and the same total number of atoms N. Periodically, the global system is in a separable state: with *exchanged* occupation numbers at times $T_l = \frac{\pi}{\lambda}\left(l + \frac{1}{2}\right)$; and with the *same* occupation numbers for the period $\tau_1 = \frac{\pi}{\lambda}$. This would predict a *population oscillation* in the two-species BECs, where the period of such oscillation would be determined by the external laser intensity used to produce the Raman transition responsible for the Josephson coupling. We have also shown that for a large excitation number $N \gg 1$ (this would be the case of two BECs), the entanglement of the subsystems becomes faster, and the value of the von Neumann entropy increases at the maximum entropy times as we increase N. In this case, the results *do not* depend either on the nonlinear coupling parameter g or on the Planck constant, and the semiclassical limit corresponds to the large N limit.

In the case of a separable product of *coherent states*, the scenario would be more appropriate for two electromagnetic field modes interacting in Kerr-type media, for instance in a Mach–Zehnder interferometer. For this situation, our results show that the interaction responsible for the entanglement of subsystems is the biquadratic one (cross-Kerr). We have determined the general purification times associated with the nonlinear coupling term $T_l = l\frac{\pi}{\hbar g}$, where for *odd* l the system goes to a product of coherent states π-rotated with respect to the original ones, whereas for *even* l the system returns to the initial product state. We have also shown that the entanglement between the two subsystems prevents the appearance of superpositions of n-coherent states in each bosonic mode for integer fractions of the purification period $\frac{T_1}{n}$ [19]. Instead, we have shown that at these fractions of the purification times, mixtures of n Schrödinger cat states are formed. The *dynamical generation of Schrödinger cat states* in one of the bosonic modes is still possible in this case, if the initial values of α_1 and α_2 are chosen appropriately, and these new purification times are dictated by the relation between the bilinear coupling λ and the nonlinear coupling g. At these times, one of the subsystems evolves to a superposition of coherent states, whereas the other goes to the subsystem vacuum state.

Finally, we show, in the semiclassical limit $\left(\frac{\hbar}{\Lambda} \to 0\right)$ of initially separable coherent states, how two things happen: first, both the purification and the recurrence times *go away* and the entanglement process becomes *irreversible* for all practical purposes; second, the break time t_b of two different regimes of entanglement corresponds to the known *Ehrenfest scale* of the model. This indicates that the short time dynamics of this model is mainly governed by the classical flow. In conclusion, we have treated a simple, integrable case of the two-mode model, but despite this, we have been able to show the mechanisms of occurrence of many interesting effects such as population oscillations, generation of Schrödinger cats and how the Ehrenfest scale and irreversibility appear in the semiclassical limit. These effects could be present in different physical contexts for more realistic cases.

Acknowledgments

The authors acknowledge K M Fonseca Romero for helpful discussions and Conselho Nacional de Desenvolvimento Científico e Tecnológico (CNPq) (contracts no 300651/85-6, no 146010/99-0) and Fundação de Amparo à Pesquisa de São Paulo (FAPESP) (contract no 98/13617-4) for financial support.

Appendix. A demonstration of a mixture of Schrödinger cat states

We first rewrite equation (14) in a more compact notation

$$|\psi(t)\rangle = \sum_{n,m} c_n(\gamma_1)c_m(\gamma_2)\,\mathrm{e}^{-\mathrm{i}g\hbar t(n+m)^2}\,|n,m\rangle \tag{A.1}$$

$$c_n(\gamma) = \mathrm{e}^{-\frac{|\gamma|^2}{2}}\frac{\gamma^n}{\sqrt{n!}} \tag{A.2}$$

where $\gamma_k = \beta_k\,\mathrm{e}^{-\mathrm{i}2g\hbar t}$ and β_k are functions of time. We are interested in the instance $t_{r,s} = \frac{\pi}{g\hbar}\frac{r}{s} = T_1\frac{r}{s}$, where r and s are mutually prime with $r < s$. Then, using the discrete Fourier transform [35]

$$\mathrm{e}^{-\mathrm{i}\pi n^2\frac{r}{s}} = \sum_{q=0}^{l-1} a_q^{(r,s)}\,\mathrm{e}^{-\mathrm{i}2\pi n\frac{p}{l}} \tag{A.3}$$

where

$$l = \begin{cases} s & \text{if } r \text{ is odd and } s \text{ is even, or vice versa} \\ 2s & \text{if both } r \text{ and } s \text{ are odd;} \end{cases} \tag{A.4}$$

and

$$a_q^{(r,s)} = \frac{1}{l}\sum_{k=0}^{l-1}\mathrm{e}^{-\mathrm{i}\pi k(k\frac{r}{s}-2\frac{q}{l})}. \tag{A.5}$$

Using the above equations, we rewrite equation (A.1) for the mentioned instances as follows:

$$\begin{aligned}|\psi(t_{r,s})\rangle &= \sum_{n,m} c_n(\gamma_1)c_m(\gamma_2)\,\mathrm{e}^{-\mathrm{i}\pi\frac{r}{s}(n+m)^2}|n,m\rangle \\ &= \sum_{q,p=0}^{l-1} a_q a_p \sum_{n,m} c_n(\eta_{1q}\,\mathrm{e}^{-\mathrm{i}2\pi m\frac{r}{s}})c_m(\eta_{2p})|n,m\rangle \\ &= \sum_{q,p=0}^{l-1} a_q a_p \sum_{m} |\eta_{1q}\,\mathrm{e}^{-\mathrm{i}2\pi m\frac{r}{s}}\rangle \otimes c_m(\eta_{2p})|m\rangle \\ &= \sum_{m} |\mathcal{C}_m\rangle \otimes \sum_{p=0}^{l-1} a_p c_m(\eta_{2p})|m\rangle \end{aligned} \tag{A.6}$$

where $\eta_{kq} = \gamma_k\,\mathrm{e}^{-\mathrm{i}2\pi\frac{q}{l}} = \beta_k\,\mathrm{e}^{-\mathrm{i}2\pi\left(\frac{q}{l}+\frac{r}{s}\right)}$, and we have defined the following cat-like states for the oscillator-1

$$|\mathcal{C}_m\rangle = \sum_{q=0}^{l-1} a_q|\eta_{1q}\,\mathrm{e}^{-\mathrm{i}2\pi m\frac{r}{s}}\rangle. \tag{A.7}$$

Then, by constructing the global density operator and tracing over the oscillator-2, i.e., summing over the remaining Fock states, we finally get the following mixture of cat states:

$$\rho_1(t_{r,s}) = \sum_m \xi_m |\mathcal{C}_m\rangle\langle\mathcal{C}_m| \tag{A.8}$$

$$\xi_m = \sum_{p,p'=0}^{l-1} a_p a_{p'}^* c_m(\eta_{2p}) c_m^*(\eta_{2p'}). \tag{A.9}$$

Using a similar procedure, we can rewrite equation (31) as a superposition of coherent states. If the condition $\hbar g t_1 = \frac{r}{s}$ verifies, we can again use the discrete Fourier transform, equation (A.3), and rewrite equation (31) as

$$|\psi_1(t_1)\rangle = \sum_{q=0}^{l-1} a_q^{(r,s)} |\beta_1(t_1)\, \mathrm{e}^{-2\pi \mathrm{i} \frac{q}{l}}\rangle \tag{A.10}$$

where $a_q^{(r,s)}$ is given by equation (A.5).

References

[1] Werner R F 2001 *Quantum Information (Springer Tracts in Modern Physics vol 173)* (Heidelberg: Springer)
[2] Braunstein S L and Kimble H J 1988 *Phys. Rev. Lett.* **80** 869
Furusawa A *et al* 1998 *Science* **282** 706
[3] Ralph T C 2000 *Phys. Rev.* A **61** 010303 (R)
Grosshans F and Grangier P 2002 *Phys. Rev. Lett.* **88** 057902
Silberhorn Ch *et al* 2002 *Phys. Rev. Lett.* **88** 167902
[4] Braunstein S L *et al* 2001 *Phys. Rev. Lett.* **86** 4938
Fiurásek J 2001 *Phys. Rev. Lett.* **86** 4942
[5] Schmidt H and Imamoğlu A 1996 *Opt. Lett.* **21** 1936
Schmidt H and Imamoğlu A 1996 *Opt. Lett.* **23** 1936
Harris S E 1997 *Phys. Today* **50** 36
Harris S E, Field J E and Imamoğlu A 1990 *Phys. Today* **64** 1107
Marangos J P 1998 *J. Mod. Opt.* **45** 471
[6] Hau L V *et al* 1999 *Nature* **397** 594
[7] Lukin M D and Imamoğlu A 2000 *Phys. Rev. Lett.* **84** 1419
[8] Deng L *et al* 2002 *Phys. Rev. Lett.* **88** 143902
[9] Imoto N, Haus H A and Yamamoto Y 1985 *Phys. Rev.* A **32** 2287
[10] Gerry C C 1999 *Phys. Rev.* A **59** 4095
[11] Leggett A J 2001 *Rev. Mod. Phys.* **73** 307
[12] Milburn G J *et al* 1997 *Phys. Rev.* A **55** 4318
[13] Sørensen A *et al* 2001 *Nature* **409** 63
[14] Micheli A *et al* 2003 *Phys. Rev.* A **67** 013607
[15] Hines A P, McKenzie R H and Milburn G J 2003 *Phys. Rev.* A **67** 013609
[16] Cirac J I, Lewenstein M, Mølmer K and Zoller P 1998 *Phys. Rev.* A **57** 1208
[17] Ruostekoskil J, Collett M J, Graham R and Walls D F 1998 *Phys. Rev.* A **57** 511
[18] Gordon D and Savage C M 1999 *Phys. Rev.* A **59** 4623
[19] Milburn G J 1986 *Phys. Rev.* A **33** 674
[20] Agarwal G S and Banerji J 1998 *Phys. Rev.* A **57** 674
[21] Opatrný T and Welsch D-G 2001 *Phys. Rev.* A **64** 023805
[22] Scully M O and Zubairy M S 1997 *Quantum Optics* (Cambridge: Cambridge University Press)
[23] Myatt C J *et al* 1997 *Phys. Rev. Lett.* **78** 586
[24] Matthews M R *et al* 1998 *Phys. Rev. Lett.* **81** 243
[25] Hall D S *et al* 1998 *Phys. Rev. Lett.* **81** 1539
Hall D S *et al* 1998 *Phys. Rev. Lett.* **81** 1543
[26] Mokarzel S G, Salgueiro A N and Nemes M C 2002 *Phys. Rev.* A **65** 044101
[27] Zoubi H, Orenstien M and Ron A 2000 *Phys. Rev.* A **62** 033801

[28] Campos R A, Saleh B E and Teich M C 1989 *Phys. Rev.* A **40** 1371
[29] Agarwal G S and Puri R R 1989 *Phys. Rev.* A **39** 2969 and references therein
[30] Angelo R M, Sanz L and Furuya K in preparation
[31] Ehrenfest P 1927 *Z. Phys.* **45** 455
[32] Berman G P, Iomin A M and Zaslavsky G M 1981 *Physica* D **4** 113
[33] Adélcio C, Oliveira, Nemes M C and Fonseca K M 2003 *Phys. Rev.* E (accepted)
[34] Angelo R M, Sanz L and Furuya K 2003 *Phys. Rev.* E **68** 016206 (*Preprint* quant-ph/0302020)
[35] Banerji J 2001 *Pramana J. Phys.* **56** 267–80